Supporting Information

Bravo-Abad et al. 10.1073/pnas.1207335109

SI Text

In the following, we present a detailed description of the theoretical treatment of the spontaneous emission coupling efficiency (the β factor) used in the main text. We start by deriving a general expression for the β factor for the class of structures considered in our work. Within the Wigner–Weisskopf approximation (1), the rate of spontaneous emission Γ of a two-level quantum emitter embedded in a complex electromagnetic (EM) environment can be described by Fermi's golden rule (2, 3)

$$\Gamma = \frac{\pi d^2 \omega_s}{\hbar \epsilon_0} \rho(\mathbf{r}_s, \hat{\mathbf{d}}, \omega_s) \qquad [S1]$$

where $\mathbf{d} = d\hat{\mathbf{d}}$ is the dipolar moment associated to the radiative transition of the emitter. Here ω_s is the frequency of that transition, whereas ϵ_0 and $\hbar$ are the vacuum permittivity and the reduced Planck's constant, respectively. The scalar function $\rho(\mathbf{r}, \hat{\mathbf{d}}, \omega)$ represents the photonic local density of states (LDOS) accessible to the emitter at position $\mathbf{r} = \mathbf{r}_s$.

On the other hand, in the case of a nondissipative system, in which the electric field can be expanded in terms of a complete basis of transverse orthonormal modes $\{\mathbf{E}_m(\mathbf{r})\}$ of frequencies $\{\omega_m\}$, the LDOS can be expressed as (3–5)

$$\rho(\mathbf{r}, \hat{\mathbf{d}}, \omega) = \sum_m \delta(\omega - \omega_m) \epsilon(\mathbf{r}) |\hat{\mathbf{d}} \cdot \mathbf{E}_m(\mathbf{r})|^2 \qquad [S2]$$

where $\epsilon(\mathbf{r})$ is the position dependent dielectric constant characterizing the system. Each of the modes in Eq. **S2** satisfies the following orthonormality condition

$$\int d\mathbf{r} \epsilon(\mathbf{r}) \mathbf{E}_m(\mathbf{r}) \mathbf{E}_n^*(\mathbf{r}) = \delta_{mn} \qquad [S3]$$

with δ_{nm} standing for the Kronecker's delta. The transversality condition reads

$$\nabla \cdot [\epsilon(\mathbf{r}) \mathbf{E}_m(\mathbf{r})] = 0 \qquad [S4]$$

Note also that each mode profile $\mathbf{E}_m(\mathbf{r})$ can be obtained by solving the following wave equation

$$\nabla \times [\nabla \times \mathbf{E}_m(\mathbf{r})] = \mu_0 \epsilon(\mathbf{r}) \omega_m^2 \mathbf{E}_m(\mathbf{r}) \qquad [S5]$$

where μ_0 is the vacuum permeability.

Now, by definition, the β-factor can be calculated as $\beta = \Gamma_t / \Gamma_{\text{all}}$, where Γ_t is the spontaneous emission rate into a given targeted mode (often a laser mode) and Γ_{all} is the total spontaneous emission rate into all the modes of the system (including the targeted one) (6). Thus, assuming that the lineshape of the emission transition is defined by function $g(\omega)$, by inserting Eq. **S2** into Eq. **S1** and integrating the resulting expression over ω, we obtain the following expression for Γ_{all}, corresponding to an emitter located at $\mathbf{r} = \mathbf{r}_s$

$$\Gamma_{\text{all}} = \frac{\pi d^2 \epsilon(\mathbf{r})}{\hbar \epsilon_0} \int d\omega g(\omega) \omega f(\omega, \mathbf{r}_s) \qquad [S6]$$

where function $f(\omega, \mathbf{r})$ is defined as

$$f(\omega, \mathbf{r}) = \sum_m \delta(\omega - \omega_m) |\hat{\mathbf{d}} \cdot \mathbf{E}_m(\mathbf{r})|^2. \qquad [S7]$$

Eqs. **S6** and **S7** summarize well the physical origin of the total spontaneous emission decay in the considered system: On the one hand, the different terms in the summand of Eq. **S7** account for the different modes in which a single frequency component ω of considered emission transition can decay to. On the other hand, the integral in ω appearing in Eq. **S6** accounts for the continuous sum of these possible radiative decay paths for all frequency components of the emission transition. Note that, as expected, the lineshape of the emission, $g(\omega)$, acts as a frequency dependent weight in this sum. The additional factor ω multiplying $g(\omega)$ in the integral of Eq. **S6** comes just from the proportionality factor that links the spontaneous emission rate and the LDOS (see Eq. **S1**).

This physical picture of the decay process also allows us to obtain an expression for Γ_t simply by singling out the contribution to Γ_{all} that stems from the considered targeted mode. In particular, if we define $\mathbf{E}_t(\mathbf{r})$ and ω_t to be the targeted electric-field profile and its corresponding frequency, respectively, the magnitude of Γ_t can be obtained by substituting $g(\omega)$ by $g_t(\omega) \equiv \delta(\omega - \omega_t)$ in Eq. **S7** and by replacing $f(\omega, \mathbf{r}_s)$ by $f_t(\omega, \mathbf{r}) \equiv \delta(\omega - \omega_t) |\hat{\mathbf{d}} \cdot \mathbf{E}_t(\mathbf{r})|^2$. This yields

$$\Gamma_t = \frac{\pi d^2 \epsilon(\mathbf{r}_s)}{\hbar \epsilon_0} \omega_t g(\omega_t) |\hat{\mathbf{d}} \cdot \mathbf{E}_t(\mathbf{r}_s)|^2. \qquad [S8]$$

Note that dividing Eq. **S8** by Eq. **S6**, and using the definition of the LDOS given in Eq. **S2**, we recover Eq. **2** of the main text.

We now focus on the application of the above formalism to calculate the β factor in the case in which the emitter is embedded in a three-dimensional photonic crystal (PhC). We assume that the considered PhC is characterized by a finite volume $V = L_x \times L_y \times L_z$ (where L_x, L_y, L_z are the dimensions of the PhC along the x, y, and z axis, respectively). Here we emphasize that in our theoretical calculations, this three-dimensional analysis is applied to the homogeneous and band-edge cases discussed in the main text. (The homogeneous case can be trivially considered as a periodic system with an arbitray periodicity). For the Dirac case, however, due to the out-of-plane subwavelength confinement of the EM fields introduced by the full photonic band gap, the analysis is performed in terms of the in-plane transverse area of the system, $A = L_x \times L_y$ (see discussion in the main text).

To analyze the finite-size effects on the β-factor, without loss of generality, we assume the volume V (or transversal area A for the Dirac case) to be surrounded by Born–von Karman boundary conditions [i.e., periodic boundary conditions (7); our theoretical analysis admits a straightforward generalization to other types of boundary conditions]. In this case, the index m used above to label the modes can be identified with $\{n, \mathbf{k}, \sigma\}$, where n is the band index, $\mathbf{k}$ is the wavevector of each Bloch mode [$\mathbf{k}$ lies inside the first Brillouin zone (FBZ)] and σ labels the polarization ($\sigma = 1$ and $\sigma = 2$, for s and p polarization, respectively). In addition, because the system is finite, $\mathbf{k}$ can only take discrete values: $\mathbf{k} = 2\pi \times (n_x/L_x, n_y/L_y, n_z/L_z)$ for the homogeneous and band-edge cases, and $\mathbf{k} = 2\pi \times (n_x/L_x, n_y/L_y, 0)$ for the Dirac case (in all three cases, n_x, n_y, and n_z are arbitrary integers). Thus, once the normal modes of the system $\mathbf{E}_{n,\mathbf{k},\sigma}$ are computed (for which we have used the plane-wave expansion method to Maxwell's equations (8), from Eqs. **S6** and **S8** the β factor can be calculated

using

$$\beta = \frac{\omega_t g(\omega_t)|\mathbf{E}_t(\mathbf{r})\cdot\hat{\mathbf{d}}|^2}{\int d\omega g(\omega)\omega\{\Sigma_{n,\mathbf{k},\sigma}\delta(\omega-\omega_{n,\mathbf{k},\sigma})|\mathbf{E}_{n,\mathbf{k},\sigma}(\mathbf{r})\cdot\hat{\mathbf{d}}|^2\}}. \quad \textbf{[S9]}$$

In the limit in which the volume V of the system is such that $V \gg \lambda^3$ (or equivalently, for the Dirac case, when the area A is such that $A \gg \lambda^2$), with λ being the central emission wavelength, semianalytical expressions for the β-factor can be obtained by assuming a continuous distribution of $\mathbf{k}$ vectors over the FBZ. Specifically, we can replace $\Sigma_{\mathbf{k}} \to V/(2\pi)^3\int_{\mathrm{FBZ}}d\mathbf{k}$ in the homogeneous and band-edge cases, and $\Sigma_{\mathbf{k}} \to A/(2\pi)^2\int_{\mathrm{FBZ}}d\mathbf{k}$ in the Dirac case (note that in all three cases the integral over $\mathbf{k}$ is performed over the whole FBZ) . Then, if we expand the argument of the Dirac delta appearing in the denominator of the right-hand side of Eq. **S9**) using

$$\omega - \omega_{n,\sigma}(\mathbf{k}_0) = \nabla\mathbf{k}_0\omega[\mathbf{k}_0 - \mathbf{k}_0(\omega_{n,\sigma})] + O(|\mathbf{k}_0 - \mathbf{k}_0(\omega_{n,\sigma})|^2) \quad \textbf{[S10]}$$

and neglect the contribution of second order terms in $|\mathbf{k}_0 - \mathbf{k}_0(\omega_{n,\sigma})|$ (6), after some straightforward algebra, one finds that Eq. **S9** can be rewritten as

$$\beta = \frac{1}{V}\frac{\omega_s g(\omega_s)}{\int d\omega g(\omega)\omega\tilde{\rho}(\omega)} \quad \textbf{[S11]}$$

where the function $\tilde{\rho}(\omega)$ determines the total density of photonic states per unit volume in the structure. Note that in the Dirac case, V must be replaced by the transversal area A. In analogy with standard analyses in solid-state physics (6), in the homogeneous and band-edge cases, $\tilde{\rho}(\omega)$ can be expressed as

$$\tilde{\rho}(\omega) = \frac{1}{(2\pi)^3}\int_{A(\omega_s)}\frac{1}{v_g}dk_t \quad \textbf{[S12]}$$

where $A(\omega_s)$ denotes the equifrequency surface $\omega = \omega_s$, and v_g is the magnitude of the group velocity $v_g = |d\omega/dk|$. At each point of the equifrequency surface, k_t stands for the component of the 3D vector $\mathbf{k}$ that lies along the tangential direction to $A(\omega_s)$ at each point of the k-space. In the Dirac case a similar expression holds for $\tilde{\rho}(\omega)$, but now the domain of integration in Eq. **S12** is a equifrequency curve instead of equifrequency surface. The resulting expressions $\tilde{\rho}(\omega)$, obtained by performing the integral defined by Eq. **S12** for the different dispersion relations considered in this work, are discussed in detail in the main text.

Importantly, in deriving Eq. **S11** we have assumed that for the range of parameters considered in this work, the emission bandwidth is narrow enough so that $|\mathbf{E}_{n\mathbf{k}\sigma}(\mathbf{r})|^2 \approx |\mathbf{E}_t(\mathbf{r})|^2$ for all modes whose equifrequencies $\omega_{n\mathbf{k}\sigma}$ lie inside the interval where $g(\omega)$ is not negligible. To verify numerically the accuracy of this approximation in the Dirac case (a similar analysis holds for the band-edge case), we have probed directly the LDOS of the 2D counterpart of the defect layer structure shown in Fig. 1*A* of the main text. Specifically, in order to do that, we have computed the power radiated by a dipole placed in the low-refractive index regions of the structure (i.e., in the interstitial regions among cylinders), $P_{\mathrm{out}}(\mathbf{r},\hat{\mathbf{d}},\omega)$. To compute $P_{\mathrm{out}}(\mathbf{r},\hat{\mathbf{d}},\omega)$ we have employed a generalization of the conventional coupled-mode theory (9), in which each Bloch mode is considered as an independent input/output channel (see details in ref. 10). The computed results are summarized in Fig. S1, in which band structure calculations (Fig. S1*A*) are displayed together with the corresponding dependence of $P_{\mathrm{out}}(\mathbf{r},\hat{\mathbf{d}},\omega)$ with frequency (Fig. S1*B*). As observed in these results, the dependence of $P_{\mathrm{out}}(\mathbf{r},\hat{\mathbf{d}},\omega)$ with ω near the Dirac frequency ω_D [and hence the LDOS (11)], obtained by assuming $|\mathbf{E}_{n\mathbf{k}\sigma}(\mathbf{r})|^2 \approx |\mathbf{E}_s(\mathbf{r})|^2$, is in good agreement with full numerical calculations within a moderately large bandwidth of frequencies (see comparison between cyan line and blue line in the bottom inset of Fig. S1*B*). Finally, we note that although in the particular case considered in Fig. S1*B* the dipole has been placed at the center of the unit cell of the triangular lattice, with $\hat{\mathbf{d}}$ pointing along the x direction (see top inset of Fig. S1*B*), we have checked that similar good agreement between numerical and and semianalytical results is obtained for other positions of the dipole in the unit cell, as well as for other orientations of $\hat{\mathbf{d}}$.

1. Scully MO, Zuibary MS (1997) *Quantum Optics* (Cambridge Univ Press, Cambridge, UK).
2. Loudon R (2000) *The Quantum Theory of Light* (Oxford Univ. Press, New York).
3. Novotny L, Hecht B (2006) *Principles of Nano-Optics* (Cambridge University Press, Cambridge, UK).
4. Busch K, John S (1998) Photonic band gap formation in certain self-organizing systems. *Phys Rev E* 58:3896–3908.
5. Sprik R, van Tiggelen BA, Lagendijk A (1996) Optical emission in periodic dielectrics. *Europhys Lett.* 35:265–270.
6. Kittel C (1976) *Introduction to Solid-State Physics* (Wiley, New York).
7. Vuckovic J, Painter O, Xu Y, Yariv A (1999) Finite-difference time-domain calculation of the spontaneous emission coupling factor in optical microcavities. *IEEE J of Quantum Electr* 35:1168–1175.
8. Johnson SG, Joannopoulos JD (2001) Block-iterative frequency-domain methods for Maxwell's equations in a planewave basis. *Opt Express* 8:173–190.
9. Haus HA (1984) *Waves and Fields in Optoelectronics* (Prentice-Hall, Englewood Cliffs, NJ).
10. Hamam R, et al. (2008) Purcell effect in nonlinear photonic structures: A coupled mode theory analysis. *Opt Express* 16:12523–12537.
11. Xu Y, Lee RK, Yariv A (2000) Quantum analysis and the classical analysis of spontaneous emission in a microcavity. *Phys Rev A* 61:033807.

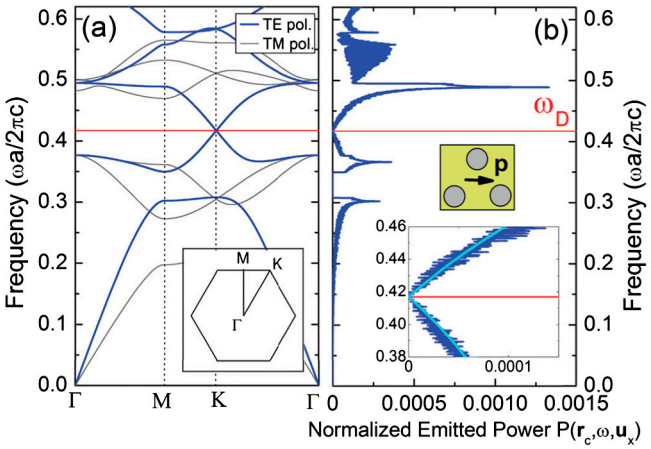

Fig. S1. (*A*) Numerical calculation of two-dimensional photonic bands displaying an isolated Dirac point. The analyzed system is formed by a triangular lattice of dielectric cylinders of refractive index $n_d = 3.1$ and radius $r_d = 0.32a$ (*a* being the lattice constant) embedded in air. (*B*) Power emitted by a dipole located at the center of the unit cell of the considered photonic crystal and with its dipolar moment pointing along the *x* axis (see sketch in top inset of this panel). In both panels, ω_D marks the frequency of the Dirac point. Bottom inset in *B* shows the comparison between the predictions of semianalytical and full numerical calculations (cyan and blue lines, respectively) for the emitted power.